Journal of Power Sources 267 (2014) 117–122

Contents lists available at ScienceDirect

Journal of Power Sources

journal homepage: www.elsevier.com/locate/jpowsour

# Evaluation of Ni and Ni–$Ce_{0.8}Sm_{0.2}O_{2-\delta}$ (SDC) impregnated 430L anodes for metal-supported solid oxide fuel cells

Yucun Zhou*, Chun Yuan, Ting Chen, Xie Meng, Xiaofeng Ye, Junliang Li, Shaorong Wang, Zhongliang Zhan

*CAS Key Laboratory of Materials for Energy Conversion, Shanghai Institute of Ceramics, Chinese Academy of Sciences (SICCAS), 1295 Dingxi Road, Shanghai 200050, PR China*

## HIGHLIGHTS

- Ni and Ni–SDC impregnated 430L anodes for MS-SOFCs are evaluated.
- Polarization resistance of the Ni–SDC-430L anode is only 0.12 Ω $cm^2$ at 650 °C.
- A 1200 h durability test is applied for the Ni–SDC-430L anode.
- The pre-coarsening process and the SDC introduction can enhance the anode stability.

## ARTICLE INFO

*Article history:*
Received 23 April 2014
Received in revised form
7 May 2014
Accepted 17 May 2014
Available online 27 May 2014

*Keywords:*
Metal-supported solid oxide fuel cell
Impregnation
Anode
Stability

## ABSTRACT

Ni impregnated 430L anodes used for metal-supported solid oxide fuel cells are prepared and evaluated. The effects of catalysts loadings and heat treatment temperatures on the anode polarization resistances are investigated. The stabilities of the Ni impregnated 430L anodes are also measured and increasing the calcination temperature can enable a much more stable anode performance. Furthermore, by applying the Ni–$Ce_{0.8}Sm_{0.2}O_{2-\delta}$ (SDC) impregnated 430L composite anode, a low polarization resistance of 0.12 Ω $cm^2$ at 650 °C is obtained. The 1200 h durability test shows that the polarization resistance of the composite anode increases from 0.12 Ω $cm^2$ to 0.3 Ω $cm^2$ during the initial 500 h while no degradation is found during the subsequent measurement.



## 1. Introduction

Solid oxide fuel cells (SOFCs) electrochemically convert the chemical energy of fuels into the electrical power in an energetically efficient and environmentally friendly manner. Traditional SOFCs consist of yttria-stabilized zirconia (YSZ) electrolytes, Ni–YSZ cermet anode and lanthanum strontium magnate (LSM) cathodes in either electrolyte- or electrode-supported configurations. Different from the common all-ceramic architecture, novel metal-supported SOFCs (MS-SOFCs) use porous alloys as the mechanical substrates for thin functional anode–electrolyte–cathode layers with many attractive advantages such as excellent structural robustness and stability, high tolerance toward rapid thermal cycling, easy stack assembling as well as low materials costs [1]. On the other hand, in order for MS-SOFCs to achieve high power densities and low degradation rates of commercial interest, several critical issues remain to be addressed such as excessive coarsening of Ni anodes and substantial metallic inter-diffusion between the alloy substrates and the Ni-anodes occurring not only during the high temperature co-firing process but also during the long-term operation at relatively low temperatures [2–5]. For example, chromium diffusion depth from CroFer22APU alloys to Ni-anodes could be as large as 60 μm when heat-treated at 1100 °C for 3 h in argon atmosphere [3], the nickel diffusion depth could also reach 60 μm even heat-treated at 800 °C for 250 h in the anode atmosphere [6]. Such anode issues would result in unacceptably low power densities and rapid performance degradations [5]. Therefore, the last decade has witnessed dramatically increased interest in the new configuration of MS-SOFCs with tremendous efforts devoted to optimizing their design and simplifying their fabrication procedure.

Low temperature thin film deposition techniques, including plasma spray method [7,8], and pulsed laser deposition (PLD) [9] have been used to form the functional ceramic layers on the

* Corresponding author. Tel./fax: +86 21 6990 6378.
*E-mail addresses:* zhouyc@student.sic.ac.cn, zhouycwf@gmail.com (Y. Zhou).

http://dx.doi.org/10.1016/j.jpowsour.2014.05.087
0378-7753/

metallic substrates to avoid excessive Ni coarsening and metallic inter-diffusion. Ceramic barrier layers such as $CeO_2$ and doped $LaCrO_3$ have been deposited to prevent metallic inter-diffusions between the metallic substrates and the Ni-containing anodes [2,3]. IMT alloy supported Ni–YSZ anode and YSZ electrolyte fuel cells with diffusion barrier layers and in-situ sintered LSCF cathodes provided a high power density of 1.064 W $cm^{-2}$ at 0.7 V (820 °C) [10]. Alternatively, the anode catalysts could also be introduced into the pre-fired anode porous backbones at relatively low temperatures by the impregnating method [11–13]. An additional benefit of the impregnated electrodes is their high catalytic activities for electrochemical reactions as enabled by their nano-scale structures [14–16]. Depositing the cathode layer directly onto the metal support maybe another solution to avoid the anode issues [17]. While such cell design require alternative cathode materials that are tolerant to the presence of Cr.

In our previous work, Ni and Ni–$Ce_{0.8}Sm_{0.2}O_{2-\delta}$ (SDC) impregnated 430L anodes were successfully applied into the MS-SOFCs and encouraging cell performances were also obtained [18,19]. For example, MS-SOFC with the structure of Ni–SDC impregnated 430L anode/YSZ electrolyte/$La_{0.6}Sr_{0.4}Fe_{0.9}Sc_{0.1}O_{3-\delta}$ (LSFSc) impregnated YSZ cathode was fabricated by tape casting, co-firing and impregnation. The maximum power density of 0.68 W $cm^{-2}$ was obtained at 650 °C and initial 190 h stability test of the single cell at 600 °C was shown with no obvious degradation [19]. However, long term stability and the micro structural evolution of such anodes were not studied. In this paper, Ni impregnated 430L symmetrical anode cells are prepared and the effect of catalysts loadings and heat treatment temperatures are investigated. Furthermore, Ni–SDC impregnated 430L anodes are applied and the long term stability of such anode is evaluated.

## 2. Experimental

The symmetrical anode cells with the structure of Ni or Ni–SDC impregnated 430L anodes|YSZ electrolytes|Ni or Ni–SDC impregnated 430L anodes were fabricated using a two-step procedure. Firstly, cell backbones – porous 430L|YSZ electrolytes|porous 430L – were prepared by the tape casting, tape lamination and co-firing methods. Commercial 430L stainless steel powders (Jing-yuan Powder Material Co., Ltd, China) and 8YSZ (Tosoh, Japan) were used as starting materials. The slurry for tape casting was ethanol-based and consisted of acrylic resin dispersants, polyvinyl butyral binders, dibutyl phthalate plasticizer and other organic additives in addition to alloy or ceramic powders. Green tapes were obtained by casting appropriate slurries on the Mylar carrier on the tape casting machine (Lab-Cast Model TC-71LC Tape Caster, HED International, USA). The tri-layers were produced by laminating tape cast green tapes followed by co-sintering at 1300 °C for 4 h in 5% $H_2$ – 95% $N_2$ [19]. Secondly, the anode catalysts, Ni or Ni–SDC, were impregnated onto the internal surfaces of the porous 430L backbones. Specifically, aqueous solution containing $Ni(NO_3)_2$ or $Ni(NO_3)_2$, $Sm(NO_3)_3$ and $Ce(NO_3)_3$ in stoichiometric ratios (the mass ration of SDC:Ni = 8:2) were impregnated and calcinated at 600 °C or 850 °C for 2 h in a reducing atmosphere of 5% $H_2$ – 95% $N_2$ to convert the salts into metal oxides while avoiding excessive oxidation of the stainless steel substrates. The concentration for the Ni aqueous solution was 4 mol $L^{-1}$ while that for the Ni–SDC aqueous solution was 3 mol $L^{-1}$. The loadings of impregnated catalysts were controlled by a micro-liter syringe each time and a single impregnation–calcination cycle could yield an infiltrate loading of ≈3 wt %. The ultimate catalyst loadings were tailored by increasing the impregnation–calcination cycles. The symmetric anode cells were supported by a dense YSZ electrolyte with the thickness of ≈200 μm and the thickness of the porous 430L was ≈50 μm.

For electrochemical measurements, silver grids were applied onto the electrode surfaces and silver wires were attached as the current and voltage leads (Fig. 1). Electrochemical impedance spectra (EIS) were obtained by using an IM6 Electrochemical Workstation (ZAHNER, Germany) with the cell exposed to humidified (3%$H_2O$) hydrogen at 100 mL $min^{-1}$. EIS were collected with a 20 mV AC amplitude over the frequency range of 100 mHz–0.2 MHz. In order to evaluate the stability of the impregnated catalysts, some of these cells were operated at 650 °C for different time without current applied. Active area of the symmetric anode cell was 0.64 $cm^2$. Microstructures of the anodes were examined using Hitachi S-4800-II scanning electron microscopy.

## 3. Results and discussion

Fig. 2 shows the polarization resistances of the impregnated Ni-430L anodes (calcining at 600 °C and 850 °C) measured at 650 °C in humidified hydrogen with the Ni loadings ranging from 4 wt% to 16 wt%. The ohmic resistances due to the electrolytes and connecting wires are removed while the polarization resistances are divided by two parts to account for contributions from two symmetrical electrodes. For the impregnated Ni-430L anodes calcined at 600 °C, the Ni loading of 10 wt% exhibits the lowest polarization resistance of 2.2 Ω $cm^2$. Such results are extraordinarily large compared to the Ni impregnated doped $LaGaO_3$ anode, which only exhibit a low polarization resistance of 0.008 Ω $cm^2$ at 650 °C [20]. This is very likely since the triple-phase boundaries, where the gas species meet the electronic conductors and the oxide-ionic conductors, are only confined to the narrow YSZ–Ni contact area closed to the YSZ electrolyte due to the absence of oxide-ion conducting components in the impregnated Ni-430L anodes. Note that both the polarization resistances of Ni loadings lower and higher than 10 wt% are much larger than that of the 10 wt% loading. It can be explained by the three-phase boundary (TPB) dependence of the impregnated loadings. Model study indicates that the total and active TPB lengths initially increase with increasing impregnation loading, reach a maximum value, and then decrease with a further increase in infiltration loading due to the contact between the impregnated nano particles [21]. Based upon Archimedes' method, the overall porosity of the porous 430L backbone prior to catalyst impregnation is around 40%. Further increasing the Ni loading would increase the gas diffusion resistances for the decrease of the anode porosity. Ni loadings dependence of the polarization resistances of the impregnated Ni-430L composite anodes calcined at 850 °C is also shown in Fig. 2. Different from the results of the

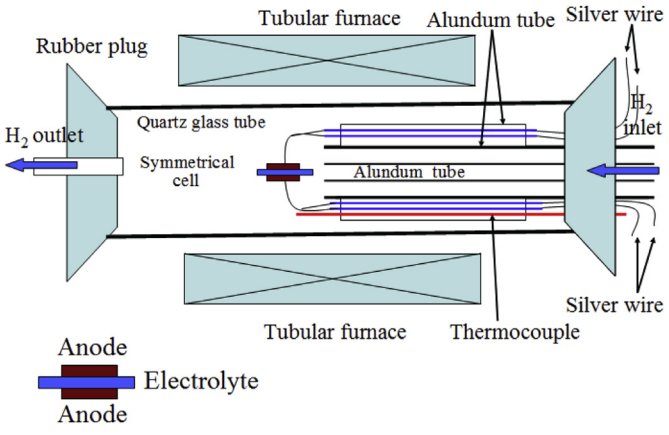


**Fig. 1.** Schematic diagram of the setup for EIS measurements.

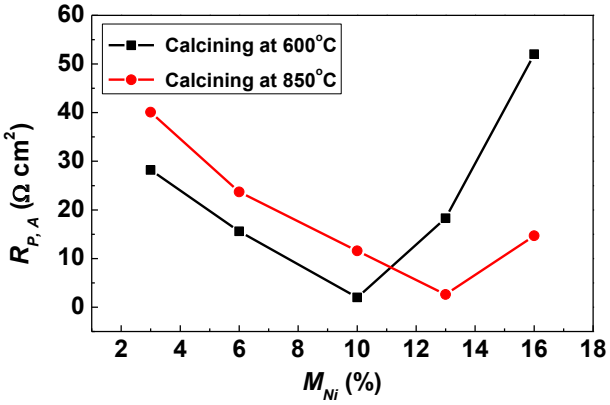


**Fig. 2.** Polarization resistances of the impregnated Ni-430L anodes calcined at 600 °C and 850 °C with different Ni loadings.

composite anodes calcined at 600 °C, the optimized loading is 13wt % for the composite anodes calcined at 850 °C. It can be explained that when the Ni particles are coarsened, connected particles tend to be isolated and increased loading is needed to provide sufficient active surfaces for the hydrogen oxidation reaction [4,18].

Impedance spectra of the impregnated Ni-430L anode (10 wt% loading) calcined at 600 °C is shown in Fig. 3(a). Notably, hydrogen oxidation kinetics is largely dominated by the charge transfer process with the summit relaxation frequency at 826 Hz, while the surface hydrogen exchange process is quick enough and makes little contributions to the anode polarization resistance since the arc commonly centered at 1 Hz is negligibly small. In order to evaluate the stability of the polarization resistance, the symmetrical anode cell was operated at 650 °C for about 50 h without current applied. The impedance spectra of the impregnated Ni-430L anode after the durability measurement is shown in Fig. 3(b). Note that the anode polarization resistance increases drastically from 2 Ω cm$^2$ to 41 Ω cm$^2$ during the 50-h measurement and an increase in the lower-frequency is shown. Such increase is much more obvious in the Bode representations of the impedance data shown in Fig. 3(c). It is reported that the higher-frequency arc is related to the charge transfer process near the TPB region, while the lower-frequency arc to the hydrogen dissociation adsorption or surface diffusion process on the Ni surface [22–25]. Since the impregnated Ni particles are easy to be coarsened [4], the coarsening of Ni particles which decreasing the density of triple-phase boundaries and active surfaces for hydrogen oxidation reactions may be the main reason to the increase of the anode polarization resistances [18,26]. A sustained increase in the polarization resistance of the impregnated Ni-430L anode during the 50-h measurement is shown in Fig. 3(d). For the unacceptable large polarization resistance after the durability test, no longer measurement was applied.

Impedance spectra of the impregnated Ni-430L anode calcined at 850 °C (13 wt% loading) before and after the stability test are shown in Fig. 4(a). A comparing of the impedance arcs in Fig. 3(a) and 4(a) (initial results) shows the similar arc shape and frequency distribution. It may exhibit that the coarsening of the Ni particles at 850 °C may not change the electrochemical process in the anode. However, the stability of the polarization resistance of the anode is improved and an increase from 2.6 Ω cm$^2$ to 4.3 Ω cm$^2$ during the 200-h measurement is exhibited in Fig. 4(a). As shown in Fig. 4(a) and (b), the increase of the polarization resistance mainly centered at the middle-frequency after the durability test. It indicates that the impregnated Ni particles may be further coarsened after the 200-h stability measurement. Compared to the rapid increase of the polarization resistance for the Ni-430L composite

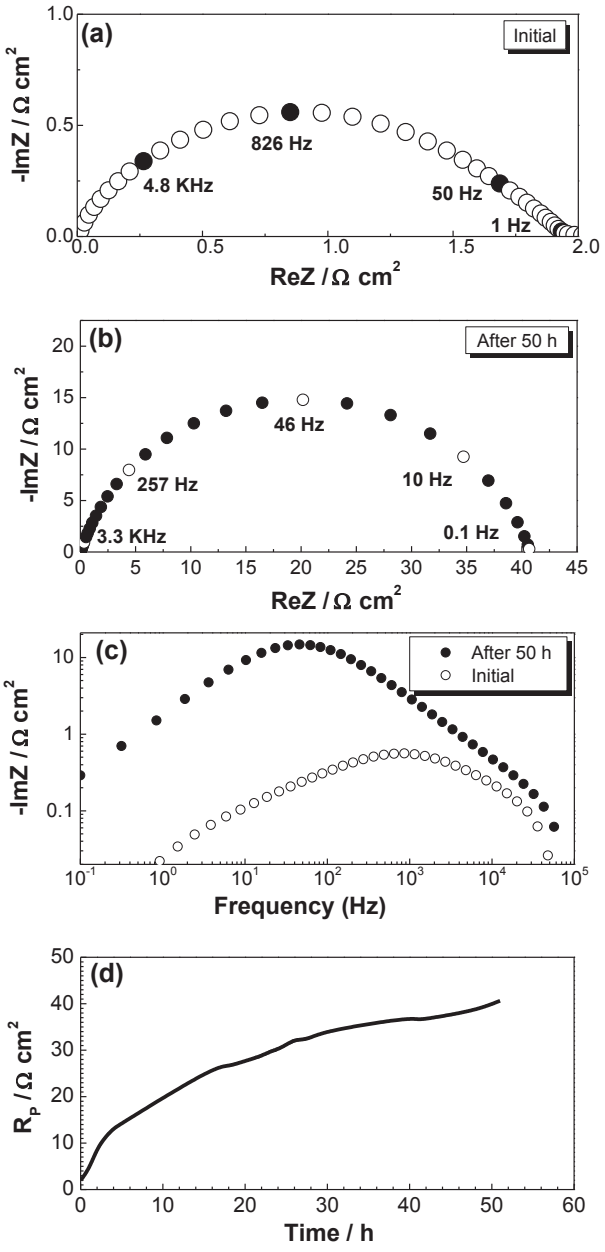


**Fig. 3.** Impedance data for the impregnated Ni-430L composite anodes calcined at 600 °C.

anode calcined at 600 °C (Fig. 3(d)), a much more slowly increase is shown in Fig. 4(c) for the anode calcined at 850 °C. This result illustrates that pre-coarsening of the Ni particles can enhance the stability of the impregnated Ni-430L anode [4].

Scanning electron microscope (SEM) images of the Ni microstructures before and after the durability measurement are shown in Fig. 5. For the Ni calcined at 600 °C, pronounced particle growth is observed. In particular, well interconnected nickel layers (Fig. 5(a)) increase to the isolated coarsening particles after the stability test (Fig. 5(b)). Such phenomenon consists with the impedance spectra change shown in Fig. 3(a) and (b). While for the Ni particles calcined at 850 °C, even the coarsening phenomenon is still observed (Fig. 5(c) and (d)), it is not so serious as that of the particles calcined at 600 °C. That may be the reason why the polarization resistance of the impregnated anode calcined at 850 °C increases more slowly with time.

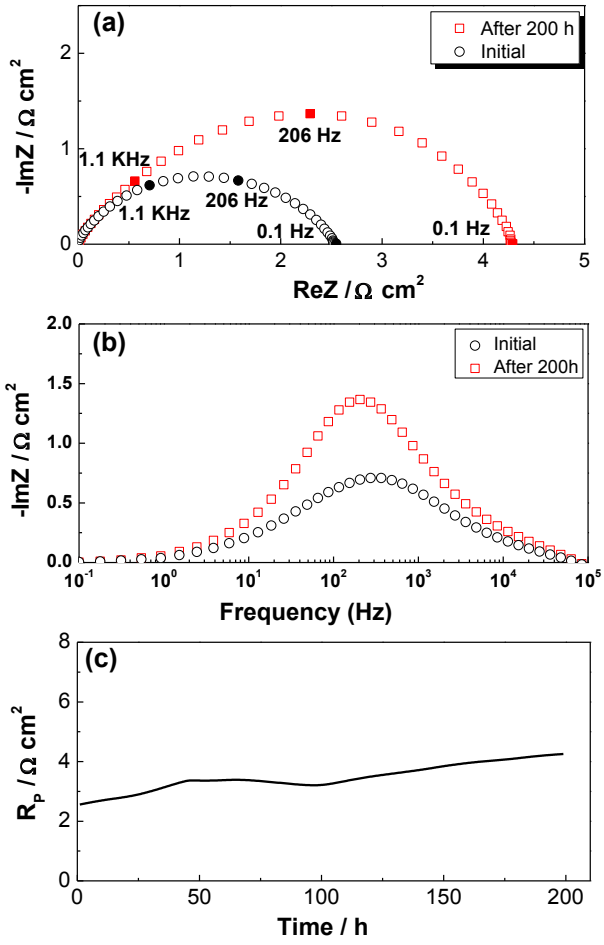


**Fig. 4.** Impedance data for the impregnated Ni-430L composite anodes calcined at 850 °C.

In order to enhance the performance and stability of the impregnated Ni-430L anode, SDC ceramic phase were added. SDC is a mixed ionic and electronic conductor (MIEC) in a reducing atmosphere and the introduction of the SDC can enlarge the active TPB lengths of the impregnated Ni-430L anode. Thus, a higher anode performance is expected. The weight ratio of SDC to Ni is chosen as 8:2. We surmise that the excessive SDC ceramic phase can restrict the growth of the Ni particles and an enhanced stability would be obtained. Since the anode loadings are optimized in the Ni impregnated 430L anode configuration as discussed above, the Ni–SDC loading of 10 wt% is applied here. Also, the calcination temperature was chosen as 600 °C.

The polarization resistance of the impregnated Ni–SDC-430L composite anode is only 0.118 Ω $cm^2$ at 650 °C (Fig. 6(a)). Such result is comparable with a Ni–CGO infiltrated FeCr–YSZ cermet anode used in another MS-SOFC, which shows a polarization resistance of 0.12 Ω $cm^2$ at 650 °C [22]. Stability of the impregnated Ni–SDC-430L composite anode is also measured at 650 °C for 1200 h. As shown in Fig. 6(b), an increase of polarization resistance from 0.12 Ω $cm^2$ to 0.3 Ω $cm^2$ is observed during the initial 500 h. After that, the polarization resistance is stabilized at around 0.3 Ω $cm^2$. Impedance spectra of the impregnated composite anode before and after the durability measurement are also shown in Fig. 6(a). Consistent with the results of the impregnated Ni-430L anode as shown above, the increase of the polarization resistance is mainly in the lower-frequency. Fig. 7 shows the SEM images of the Ni–SDC particles before and after the durability test. After the long-term test, coarsening of the particles and loss of the pores are shown. We surmise that the microstructure change would be the main reason for the increase of polarization resistance during the initial 500 h. While further extending the durability measurement may not change the microstructure and a stable polarization resistance is observed. We believe that if a pre-coarsening process is applied at the impregnated Ni–SDC-430L composite anode as that at the Ni-430L anode, a stable polarization resistance can be obtained. Considering the low operation temperature, degradation mechanisms like metallic inter-diffusion between the supporting

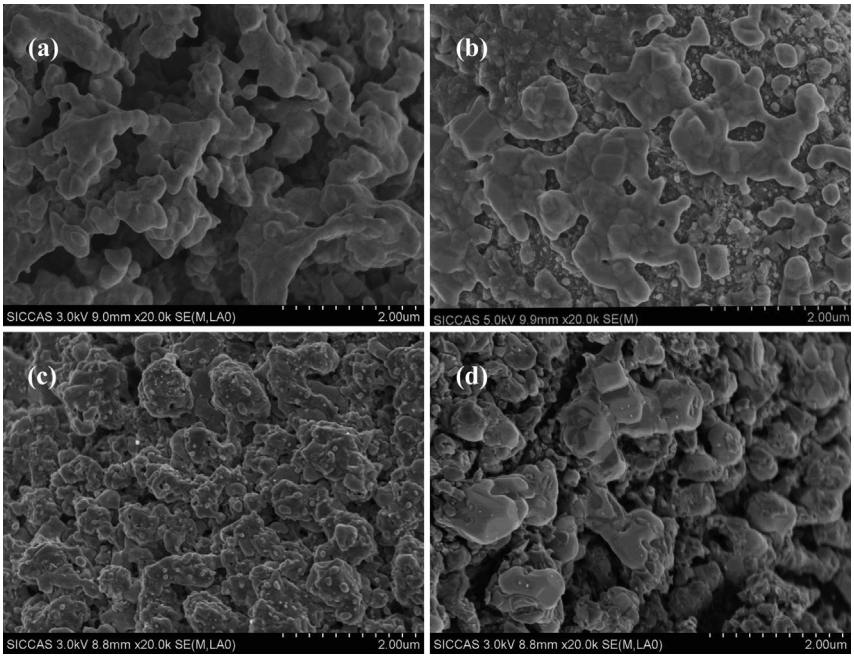


**Fig. 5.** Microstructures of the impregnated Ni particles calcined at 600 °C: (a) before and (b) after the stability test, microstructures of impregnated Ni particles calcined at 850 °C: (c) before and (d) after the stability test.

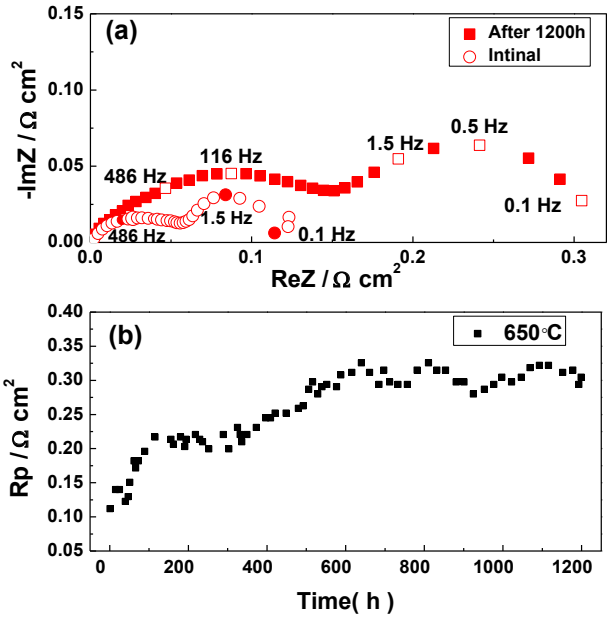


**Fig. 6.** (a) Nyquist representations of the impedance data before and after the stability test for the impregnated Ni–SDC-430L composite anodes and (b) stability of the polarization resistances measured at 650 °C.

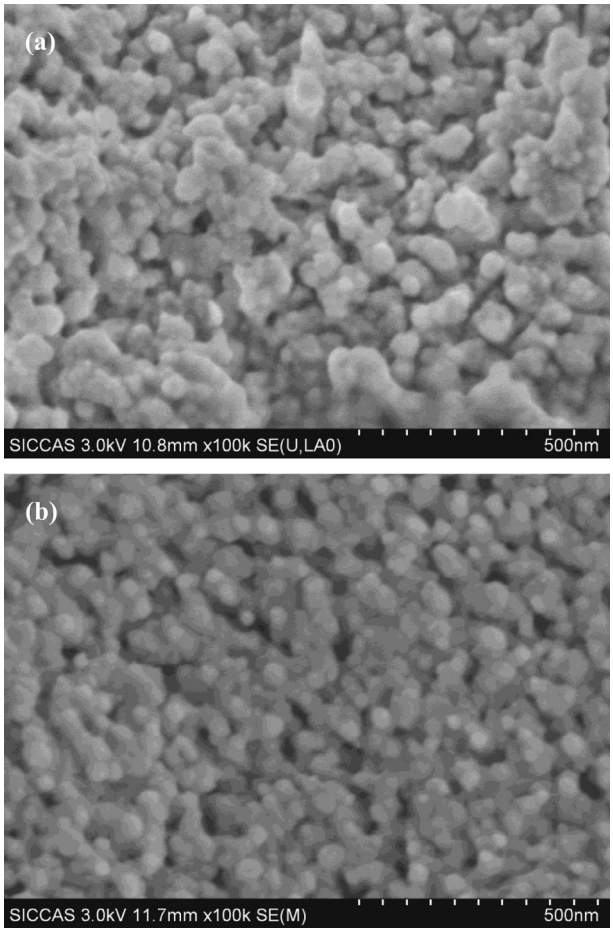


**Fig. 7.** Microstructures of the impregnated Ni–SDC particles: (a) before [16] and (b) after the stability test.

alloy substrates and the Ni anode catalysts [6,27] and oxidation of the porous alloy substrates in humidified hydrogen [28,29] may not be significant issues here.

## 4. Conclusions

Ni impregnated 430L anodes used for metal-supported solid oxide fuel cells are prepared and evaluated. The optimized loadings and the effect of heat treatment temperatures are investigated. Durability test shows a rapid increase of the polarization resistance for the Ni impregnated 430L anode calcined at 600 °C. While the stability of such anode can be enhanced by a pre-coarsening process conducted at 850 °C. Furthermore, by applying the Ni–$Ce_{0.8}Sm_{0.2}O_{2-\delta}$ (SDC) impregnated 430L anode, the polarization resistance at 650 °C can be as low as 0.12 Ω $cm^2$. A 1200 h durability test shows that the polarization resistance increase from 0.12 Ω $cm^2$ to 0.3 Ω $cm^2$ during the initial 500 h while no degradation is found during the subsequent measurement. By pre-coarsening the impregnated Ni–SDC particles, a stable polarization resistance is expected and such Ni–SDC impregnated 430L anode is appropriate to be used as the cell anode for the MS-SOFCs.

## Acknowledgment

We gratefully acknowledge the financial support from the Chinese Government High Tech Developing Project (2011AA050702), National Basic Research Program of China (No. 2012CB215400) and National Natural Science Foundation of China (No. 51172266, 51072219, 51106173, 51071169).

## References

[1] M.C. Tucker, J. Power Sources 195 (2010) 4570–4582.
[2] T. Franco, K. Schibinger, Z. Ilhan, G. Schiller, A. Venskutonis, in: K. Eguchi, S.C. Singhai, H. Yokokawa, H. Mizusaki (Eds.), Solid Oxide Fuel Cells, vol. 10, 2007, pp. 771–780.
[3] M. Brandner, M. Bram, J. Froitzheim, H.P. Buchkremer, D. Stoever, Solid State Ionics 179 (2008) 1501–1504.
[4] M.C. Tucker, G.Y. Lau, C.P. Jacobson, L.C. DeJonghe, S.J. Visco, J. Power Sources 175 (2008) 447–451.
[5] J.H. Choi, T. Lee, M. Choi, Y.-S. Yoo, S.-W. Baek, J. Bae, Int. J. Hydrogen Energy 35 (2010) 4285–4291.
[6] T. Franco, Z. HoshiarDin, P. Szabo, M. Lang, G. Schiller, J. Fuel Cell Sci. Technol. 4 (2007) 406–412.
[7] C.-S. Hwang, C.-H. Tsai, J.-F. Yu, C.-L. Chang, J.-M. Lin, Y.-H. Shiu, S.-W. Cheng, J. Power Sources 196 (2011) 1932–1939.
[8] R. Vassen, D. Hathiramani, J. Mertens, V.A.C. Haanappel, I.C. Vinke, Surf. Coat. Technol. 202 (2007) 499–508.
[9] Y.-W. Ju, T. Inagaki, S. Ida, T. Ishihara, J. Electrochem. Soc. 158 (2011) B825–B830.
[10] T. Franco, M. Haydn, R. Muecke, A. Weber, M. Ruettinger, O. Buechler, S. Uhlenbruck, N.H. Menzler, A. Venskutonis, L.S. Sigl, in: S.C. Singhal, K. Eguchi (Eds.), Solid Oxide Fuel Cells, vol. 12, 2011, pp. 343–349.
[11] M.C. Tucker, G.Y. Lau, C.P. Jacobson, L.C. DeJonghe, S.J. Visco, J. Power Sources 171 (2007) 477–482.
[12] T. Klemenso, J. Nielsen, P. Blennow, A.H. Persson, T. Stegk, B.H. Christensen, S. Sonderby, J. Power Sources 196 (2011) 9459–9466.
[13] Z. Liu, B. Liu, D. Ding, Z. Jiang, C. Xia, Int. J. Hydrogen Energy 37 (2012) 4401–4405.
[14] S.P. Jiang, Mater. Sci. Eng. A 418 (2006) 199–210.
[15] Z. Zhan, D.M. Bierschenk, J.S. Cronin, S.A. Barnett, Energy Environ. Sci. 4 (2011) 3951–3954.
[16] Z. Zhan, D. Han, T. Wu, X. Ye, S. Wang, T. Wen, S. Cho, S.A. Barnett, RSC Adv. 2 (2012) 4075–4078.
[17] D. Waldbillig, O. Kesler, J. Power Sources 191 (2009) 320–329.
[18] Y. Zhou, X. Xin, J. Li, X. Ye, C. Xia, S. Wang, Z. Zhan, Int. J. Hydrogen Energy 39 (2014) 2279–2285.
[19] Y. Zhou, X. Ye, J. Li, Z. Zhan, S. Wang, J. Electrochem. Soc. 161 (2014) F332–F336.
[20] X. Liu, X. Meng, D. Han, H. Wu, F. Zeng, Z. Zhan, J. Power Sources 222 (2013) 92–96.
[21] Y. Zhang, Q. Sun, C. Xia, M. Ni, J. Electrochem. Soc. 160 (2013) F278–F289.
[22] P. Blennow, J. Hjelm, T. Klemenso, A.H. Persson, S. Ramousse, M. Mogensen, Fuel Cells 11 (2011) 661–668.

[23] M. Chen, B.H. Kim, Q. Xu, B.G. Ahn, D.P. Huang, Solid State Ionics 181 (2010) 1119–1124.
[24] S. Jiang, S. Badwal, Solid State Ionics 123 (1999) 209–224.
[25] A. Ringuede, D. Bronin, J. Frade, Fuel Cells 1 (2001) 238–242.
[26] T.Z. Sholklapper, H. Kurokawa, C. Jacobson, S. Visco, L. De Jonghe, Nano Lett. 7 (2007) 2136–2141.
[27] T. Franco, R. Ruckdäschel, M. Lang, G. Schiller, P. Szabo, in: CD of the 7th European, Lucerne, 2006, p. 0802.
[28] S. Molin, B. Kusz, M. Gazda, P. Jasinski, J. Power Sources 181 (2008) 31–37.
[29] R. Knibbe, H.-J. Wang, P. Blennow, K. Thydén, Å.H. Persson, L. Mikkelsen, T. Klemensø, J. Power Sources 228 (2013) 75–82.